A Gallium-Nitride Switched-Capacitor Circuit Using Synchronous Rectification

Mark J. Scott, Ke Zou, Jin Wang*
The Ohio State University
Department of Electrical and Computer Engineering
Columbus, OH, USA
*wang@ece.osu.edu

Chingchi Chen, Ming Su, Lihua Chen
Ford Motor Company
Ford Research Laboratories
Dearborn, MI, USA

***Abstract*—The promise of wide band-gap materials has the potential to usher in a new era of power electronics not seen since the introduction of the Silicon (Si) Metal Oxide Semiconductor Field Effect Transistor (MOSFET) and Bipolar Junction Transistor (BJT). The physical characteristics of Gallium Nitride (GaN) make it theoretically superior to Si in such aspects as temperature of operation, switching speed, and efficiency. While much research has been conducted on the High Electron Mobility Transistor (HEMT) made of GaN and Aluminum Gallium Nitride (AlGaN), the discussion of third quadrant operation is sparse. Furthermore, the merits of the AlGaN/GaN HEMT, in particular its switching speed, make it suitable for switched-capacitor circuits. Thus, this paper focuses on the AlGaN/GaN HEMT's third quadrant operation and demonstrates this functionality in a switched capacitor circuit.**

I. INTRODUCTION

The demands placed upon power electronic equipment are growing due to increasing strain resulting from both environmental and economic concerns. The desire for hardware that can operate under higher temperatures and with greater efficiency are two reasons why devices constructed from wide band-gap semiconductors are becoming an increasingly more attractive alternative to their Silicon (Si) counterparts [1]-[6].

Gallium Nitride (GaN) is one material that has the potential to replace Si in power electronic switches [1]-[3],[5]. In several respects, GaN is superior to Si. The band-gap of GaN (3.4 eV) is three times higher than Si (1.1 ev), allowing GaN to operate at higher temperatures [1],[2],[7]. Furthermore, the critical Electric Field of GaN is over 3MV/cm compared to 0.2~0.3MV/cm of Si, and this translates into higher breakdown voltages [1],[2],[6]-[8] for similar drift region spacing (i.e. gate to drain spacing), or lower specific on-resistance for devices of comparable voltage rating. GaN also has a higher saturation velocity when compared to Si and should therefore be able to reach higher switching speeds [6].

Two common figures of merit for power conversion equipment (peFOM) are power density and efficiency. Given the characteristics listed above, GaN should enable one to realize designs that outperform Si in these respects. Higher power densities can be achieved due to two factors. First, a higher operating temperature enables the use of smaller heatsinks [3]. Second, higher switching speeds lead to smaller sized passive components [2],[9]. With regards to efficiency, improvements are achieved through lowering on resistances that result from the smaller device sizes, specifically gate to drain spacing.

The volume of literature on GaN High Electron Mobility Transistors (HEMT) is quite large. However, in relation to power electronics, there are two areas in need of further research. The first is the nature of third quadrant operation in HEMTs, and its application in synchronous rectification (SR). In a conventional GaN HEMT, the current movement through the channel created by the two dimensional electron gas (2DEG) is unipolar in nature. As a result, minority carriers are not involved in this process and the reverse recovery charge (Q_{RR}) is zero [8]. On the contrary, third quadrant current flow in a Si power MOSFET does involved minority carriers and has a reverse recovery phenomenon associated with it. The large di/dt's produced during the reverse recovery period can cause power loss and electromagnetic interference (EMI) in SR topologies [10],[11].

Panasonic has demonstrated third quadrant operation (i.e. synchronous rectification) for the commutation current in a three phase inverter circuit [5],[6]. However, this mechanism should be explored in greater detail to determine if the GaN HEMT can be used in applications where the body diode in the Si power MOSFET prohibits its use.

Switched-capacitor circuits using GaN HEMTs are another area in need of investigation because these circuits seem well suited for wide band-gap devices [12], [13]. The material's higher operating speeds means that smaller power conversion equipment can be realized since the capacitance used for energy transfer can be reduced. Additionally,

978-1-4577-0541-0/11/$26.00 ©2011 IEEE

researchers have been turning to switch-capacitor circuits to operate in higher temperature environments [12] where wide band-gap devices, theoretically, have an advantage.

The structure of this paper is as follows. Section II provides an overview of third quadrant operation and presents I-V curves for reverse current flow. Section III contains the analysis on a soft-switching, modular, switch-capacitor structure. The design of a GaN switched capacitor circuit and its performance are provided in section IV. The EPC-1010 [14], a GaN HEMT from Efficient Power Conversions, was used to perform all of the following testing.

II. Third Quadrant Testing

Knowledge of a devices' third quadrant operation is important for several reasons. Inverter circuits, for example, need a path for the commutation current to flow. However, devices such as the Silicon Carbide (SiC) Junction Field Effect Transistors (JFETs) and Si Insulated Gate Bipolar Transistors (IGBTs) do not have a means to conduct reverse current flow like the Si power MOSFETs. Therefore, an external Schottky Barrier Diode (SBD) is inserted in anti-parallel with the switch to enable the current to free-wheel in inverter circuits. If designers are able to eliminate the SBD in circuit topologies using GaN HEMTs, like Panasonic has done [5],[6], it could save manufacturers significant amounts of money over the life cycle of a product. Another advantage of third quadrant operation is that its implementation in synchronous rectification (SR) can improve the efficiency of certain topologies [9],[10].

Third quadrant current has two different paths to flow through in a Si- MOSFET. When the Gate-to-Source Voltage (V_{GS}) is below the threshold voltage (V_T), current flows through the p-n junction (i.e. body diode) created by P-base and N-drift regions that form the parasitic bipolar junction transistor (BJT) found in power MOSFETs [9]. During this time, the voltage drop across the source-to-drain (V_{SD}) will be on the order of 0.7 V. However, if V_{GS} is greater than V_T, the current can flow through the channel of the device. In this case, V_{SD} will be determined by

$$V_{SD} = I_{SD} \bullet R_{DS_ON} \quad (1).$$

Current flow across the p-n junction of the body-diode involves minority carriers, and so a reverse recovery charge (Q_{RR}) is needed to return the device to a blocking state. Even with synchronous rectification, this charge cannot be eliminated because deadtime between switching cycles is required in most power converters (Z-Source topologies being an example of where it is not).

Third quadrant current moves through EPC's GaN HEMT differently than the Si-MOSFET. As the drain voltage drops below the gate voltage, electrons begin to gather under the gate. Once the gate-to-drain voltage exceeds the threshold voltage, the channel will be turned on, and current will be able to move through the device [8].

All conduction, aside from leakage currents, flows within the 2DEG, regardless of the direction. With no minority carriers involved in this process, there is no associated Q_{RR} with EPC devices [8]. This is particularly relevant, because the rapid di/dt during the reverse recovery period can cause oscillation among those parasitic components in a circuit.

The schematic shown in Fig. 1 was used to characterize the GaN HEMT. A voltage was applied across the source-to-drain terminals of the HEMT, and two Fluke 87 V multimeters were used to measure the current (I_{SD}) and voltage (V_{SD}). During this test, the voltage was applied for one second, and then removed for 30 seconds. This period of 'rest' was necessary to minimize the rise in junction temperature.

Fig. 2 shows the results from this testing. As the voltage V_{GS} increases, the V_{SD} corresponding to a given current decreases. Thus, one is able to lower the voltage drop across the source-to-drain connection during third quadrant operation. In Fig.2 (a), the current was limited to 1 A. Since the devices were operating between the linear and saturated regions, the power loss across the device (during higher current testing) was generating enough heat to contribute to some inaccuracies in the measurements.

III. Switched-Capacitor Circuit Design

The authors have already presented a switched-capacitor voltage doubler that enjoys the benefits of minimized output capacitance and soft-switching capability [13]. Fig.3 shows the topology of the dc-dc voltage doubler. It consists of two half-cells (also called Marx cells [15]). The stray inductance from the associated PCB traces (L_{SX}) is utilized to achieve zero-current-switching (ZCS). In this topology, the location of the dc source and the load can be interchanged to achieve different types of functionality. For this application, the dc source is placed in the middle so the switches in the two cells experience the same charging current stress.

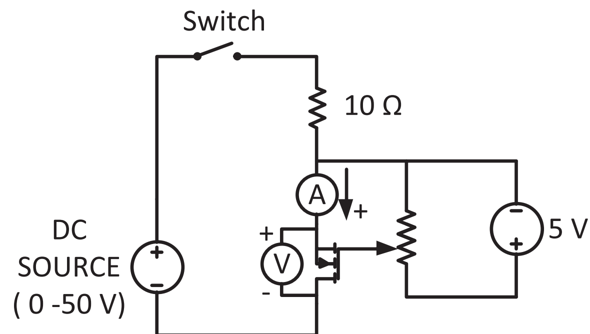

Fig. 1. Third-quadrant test circuit
(voltage and current measurements made with Fluke 87V).

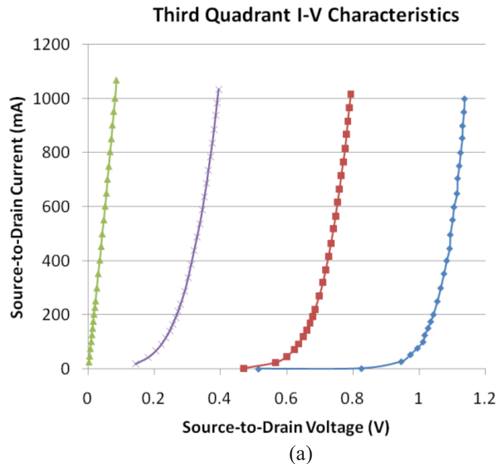

(a)

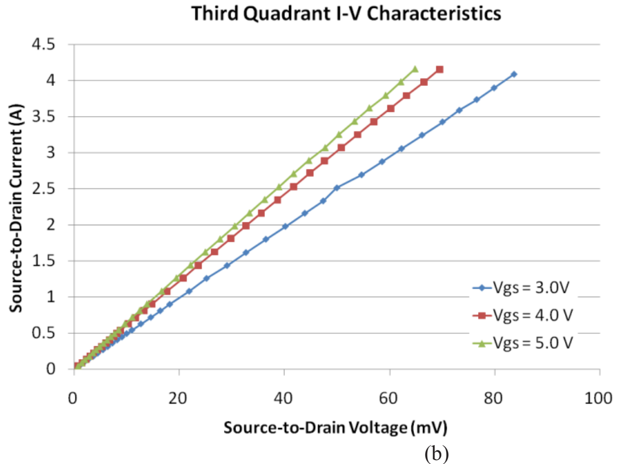

(b)

Fig. 2. EPC-1010 Third-quadrant I-V characteristics (a) low gate bias region (b) high gate bias region

Fig.6 and Fig.7 show the two switching states of this converter. During State I, the capacitor in the left cell, capacitor C_1, is being charged by the dc source through S_1 and S_2. While in the right cell, S_6 connects capacitor C_2 in series with the dc source and discharges to the load in series with the dc source, so the output voltage equals two times the dc source voltage. In State II, S_3 is turned on in the left cell and C_1 is connected in series with C_{in} to achieve the voltage doubler function. S_4 and S_5 are on for the right cell so C_2 can be charged by the dc source.

The blue-colored MOSFETs (S_2 and S_4) operate in the third quadrant, while the two other MOSFETs used for capacitor charging (S_1 and S_5) operate in the first quadrant. It can be seen in Fig.6 and Fig.7 that MOSFETs S_1 and S_5 carry just the capacitor charging current I_C, while the two third-quadrant operated MOSFETs need to carry both I_C and the load current I_R.

The stray inductance of the capacitor charging loop oscillates with the capacitors C_1 and C_2 during the charging cycle to generate a sinusoidal-shape capacitor charging current. Soft-switching is achieved by selecting the switching frequency that corresponds to the switches turning off at the zero-crossing of the charging current I_C. Thus, S1 and S5 are able to achieve ZCS. For S2 and S4, the remaining load current will free-wheel through the body diodes of the MOSFETs, and so they are turned off under a minimum voltage condition, thereby realizing zero-voltage-switching.

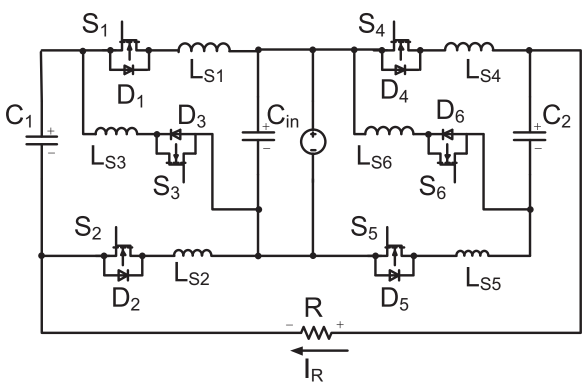

Fig. 3. A dc-dc voltage doubler based on two half-cells.

IV. Experimental Results

Fig.8 show the initial prototype of the GaN HEMT switched-capacitor voltage doubler, which was realized with EPC-1010. The topology in Fig. 3 was selected for two reasons. First, it is a modular structure. Different levels of voltage multiplication or division can be achieved by

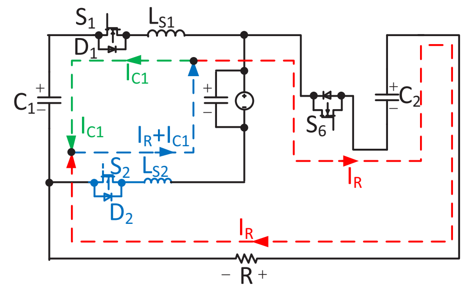

Fig. 4. The equivalent circuit of State I: C_1 is charged.

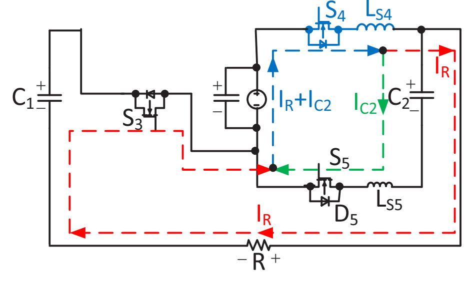

Fig. 5. The equivalent circuit of State II: C_2 is charged.

interconnecting a number of different cells. This structure also enables the realization of both dc/dc conversion and dc/ac inversion. Second, with the work presented in [13], a platform now exists where the peFOM of the Si version can be compared to those of a wide band-gap device.

The dimensions for this prototype are 4” x 3.125” x 2”. The capacitance of C_1 and C_2 is 3.0 uF, while 7.0 uF was used for C_{IN}. From Fig 7, it can be seen that the switching frequency is around 300 kHz. Using (2), the stray inductance was estimated to be 90 nH.

$$f = \frac{1}{2\pi\sqrt{LC}} \quad (2)$$

Two additional wires were inserted into the circuit at L_{S1} and L_{S5} to facilitate the measurement and display of the resonant charging current. This contributed significantly to the circuits overall stray inductance. However, this was necessary because the noise created from parasitic capacitance and inductance in the current shunt (TO-220 package in Fig. 6) drowned out the current measurement from this resistor. The ringing seen during the switching transitions is caused by the output capacitance of the GaN device resonating with the stray inductance. The oscillation frequency of this ringing was close to 30 MHz, which is the value that is obtained if the stray inductance (90 nH) and the output capacitance of HEMT (310 pF) are used in (2).

The test setup for this experiment is shown in Fig 8. Six Fluke 87 V multimeters were used during the efficiency testing. Two were used for voltage (both input and output) measurements, two for current, and two of them were used to monitor the temperature under the heatsinks. An additional meter was used to monitor the voltage supplied to the control logic and gate drive power supplies.

A Tektronix MSO 4054 was used to record the switching waveforms with the aid of two differential probes and two current probes. A Tektronix TPS 2024 was used to monitor both the drain-to-source voltage and gate-to-source voltage of the GaN HEMTs because the channels are isolated.

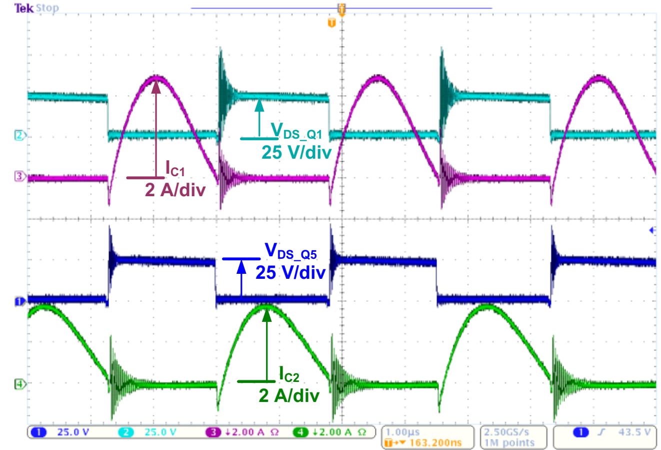

Fig. 7. Switching waveforms for the GaN HEMT switched capacitor converter (Vin = 25 V)

The efficiency test was performed by setting the input voltage to a fixed value, and then incrementing the load current from 0 to 2.5 A. The converter achieved an output power 125 W with an input voltage of 25 V. However, the maximum efficiency occurred at 75 W and was 96.4 %. The results from this testing are shown in Fig. 9. Included in the figure are two sets of efficiency values; the lower one contains the 1.2 W of loss associated with the control logic and gate drive circuitry.

Table 1 presents a comparison between the voltage doubler created from a Si MOSFET, and one created from EPC-1010 GaN HEMT. While the two platforms are not yet a fair comparison, this design was able to decrease the storage capacitor size and increase the switching frequency.

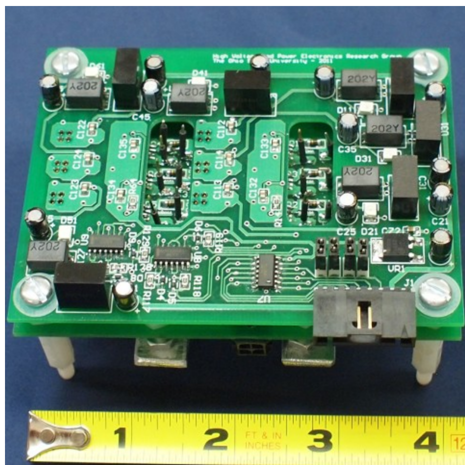

Fig. 6. The GaN HEMT switched-capacitor prototype.

Fig. 8. Setup used to test the GaN HEMTswitched-capacitor.

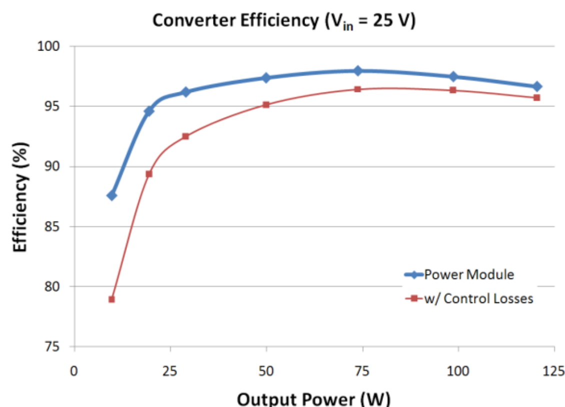

Fig. 9. Efficiency of the GaN HEMT switch-capacitor converter.

TABLE I. VOLTAGE DOUBLER COMPARISION

Parameter	dc/dc Converter Power Switch	
	IRFI4410	***EPC-1010***
Power	2 kW	125 W
Peak Efficiency	98 %	96.4%
Energy Storage Caps	47 uF	3 uF
Switching Speed	70 kHz	300 kHz

V. Conclusion

The emergence of wide band-gap power switches will continue to open up new fields of research for the power electronics designer. Synchronous rectification is one area where the GaN HEMT could be heavily utilized. This paper examined the third-quadrant capabilities of the EPC-1010 and demonstrated that the application of a gate bias will lower voltage drop across the source-to-drain terminals during reverse current flow.

This knowledge was applied in the application of a GaN-HEMT switched-capacitor prototype. The unit successfully doubled an input voltage of 25 V while carrying a load of 125 W. This prototype further demonstrates that AlGaN/GaN HEMTs can be used as synchronous rectifiers at low power levels.

VI. Acknowledgment

The authors would like to thank the manufacturing and engineering staff at Vanner Incorporated for their assistance in fabricating the PCBs for this project. In particular, we appreciate the support provided by Alec Cook, Brenda Porter, and Barry Whittington.

We also would like to thank Efficient Power Conversion for their support, specifically Alex Lidow, Steve Colino, and Bhasy Nair.

References

[1] N. Ikeda et al., "GaN Power Transistors on Si Substrates for Switching Applications," *Proceedings of the IEEE* , vol.98, no.7, July, pp. 1151-1161, 2010.

[2] M. Khan et al., "New Developments in Gallium Nitride and the Impact on Power Electronics," *IEEE Power Electronics Specialists Conference,* 2005, pp. 15-26.

[3] D. Ueda et al., "Present and future prospects of gan-based power electronics," *Solid-State and Integrated-Circuit Technology*, 2008, pp. 1078-1081.

[4] T. Funaki, M. Matsushita, M. Sasagawa, T. Kimoto, T. Hikihara, "A Study on SiC Devices in Synchronous Rectification of DC-DC Converter," *Applied Power Electronics Conference and Exposition, 2007*, pp. 339-344.

[5] T. Morita et al, "99.3% Efficiency of Three-Phase Invert for Motor Drive Using GaN-base Gate Injection Transistors," *Applied Power Electronics Conference and Exposition, 2011,* pp. 481-484 .

[6] M. Ishida, Y. Uemoto, T. Ueda, T.Tanaka, D. Ueda, "GaN Power Switching Devices," *International Power Electronics Conference,* 2010, pp 1014-1017.

[7] U. Mishra, P. Parikh, Y. Wu, "AlGaN/GaN HEMTs – an overview of device operation and applications," *Proceedings of the IEEE,* vol. 90, no. 6, June, pp.1022-1031, 2002.

[8] S. Colino, R. Beach,"Fundamenta's of Gallium Nitride Power Transistors,"Application Note," [Online] Available: http://epc-co.com/epc/documents/producttraining/Appnote_GaNfundamentals.pdf [Accessed Oct. 10, 2010]

[9] Y. Liang, R. Oruganti, T. Oh, "Design considerations of power MOSFET for high frequency synchronous rectificaion," *IEEE Transactions on Power Electronics*, vol. 10, no. 3, May, pp 388-395, 1995.

[10] N. McNeill, R. Wrobel, P. Mellor, "Synchronous rectification technique for high-voltage single-ended power converters," *IEEE Energy Conversion Congress and Exposition (ECCE), 2010* pp. 264-271.

[11] A. Fernandez, J. Sebastian, M. Hernando, P. Villegas, D. Lamar, "Using synchronous rectification for medium voltage applications," *IEEE Power Electronics Specialists Conference, 2004*, pp. 1487-1493.

[12] Q. Wei, F. Peng, L. Tolbert, "Development of a 55 kW 3X dc-dc converter for HEV systems," *IEEE Vehicle Power and Propulsion Conference, 2009*, pp. 433-439.

[13] K. Zou, M.Scott and J. Wang, "Switched Capacitor Cell Based Dc-dc and Dc-ac Converters," *Applied Power Electronics Conference and Exposition, 2011*, pp. 224-230.

[14] Efficient Power Conversion, "EPC-1010 Enhancement Mode Power Transistor," EPC-1010 Datasheet, April 2010.

[15] J.I.Rodriguez and S.B.Leeb, "A Multilevel Inverter Topology for Inductively Coupled Power Transfer," *IEEE Trans. Power Electron.*, vol. 21, no. 6, pp. 1607-1617, Nov.2006.